COMPDYN 2015
5th ECCOMAS Thematic Conference on
Computational Methods in Structural Dynamics and Earthquake Engineering
M. Papadrakakis, V. Papadopoulos, V. Plevris (eds.)
Crete Island, Greece, 25–27 May 2015

SEMI-ANALYTICAL REDUCED-ORDER MODELS FOR THE UNSTEADY AERODYNAMIC LOADS OF SUBSONIC WINGS

Marco Berci

University of Leeds
LS2 9JT, Leeds, UK
M.Berci@leeds.ac.uk

Keywords: Unsteady Loads, Subsonic Aerodynamics, Gust Response, Finite Wings.

Abstract. *Different semi-analytical reduced-order models for calculating the unsteady aerodynamic loads of subsonic slender wings are proposed. The lift-deficiency functions due to a unitary step change in the angle of attack and a unitary sharp-edged vertical gust are first obtained in the (reduced) time domain for both elliptical and rectangular wings of arbitrary aspect ratio, based on previous fundamental works available in the literature. Nonlinear optimisation is then employed to find their best analytical approximation as a series of exponential functions with optimal time constants and amplitudes, as intensively sought for efficient computations of the wing loads as well as aeroelastic stability analyses, especially in the context of aircraft's preliminary multidisciplinary design and optimisation. When the gust penetration effect is also applied, the final curve fitting is performed in the (reduced) frequency domain, where the transfer function between flow perturbation and aerodynamic load is expressed as a series of rational functions with optimal poles and gains; the approximation of the corresponding indicial function is then still obtained as a series of exponential functions with optimal time constants and amplitudes in the (reduced) time domain via Laplace transform. The optimal parameters of the lift-deficiency functions are finally tabulated and analytically expressed as function of the wing's aspect ratio, for each type of wing and flow perturbation. The obtained reduced-order models for unsteady aerodynamic loads are critically discussed and, due to their remarkable computational efficiency and theoretical insights, also suggested for suitable use in the preliminary multidisciplinary design and optimisation of flexible wings in the low-subsonic regime, characterised by attached incompressible flow.*

1 INTRODUCTION

Today's aircraft preliminary design requires a multidisciplinary approach [1] where robust and reliable aeroelastic tools as well as an effective synthesis of the model data are extremely important [2]. Suitable model reduction approaches [3-7] are hence increasingly in demand, among which fast semi-analytical calculations of the aerodynamic loads due to both aircraft motion and wind gusts are still highly desirable [8-10] for efficient aeroelastic stability analysis and structural sizing, especially in the context of wing multidisciplinary design and optimisation (MDO) [11].

For wings undergoing small variations in the effective angle of attack due to either aircraft motion or vertical gust occurrence [12], the circulatory unsteady airload due to each flow perturbation can conveniently be formulated in terms of Duhamel convolution [13] of the latter with the relative lift-deficiency indicial function [14-16]; the contributions of all flow perturbations are then linearly superposed [17-18]. Assuming incompressible potential flow [19], Wagner and Kussner derived the lift-deficiency functions due to a unitary step change in the angle of attack [20] and a unitary sharp-edged vertical gust [21-22] for a thin flat airfoil in the (reduced) time domain, respectively, while Theodorsen [23] and Sears [24-25] solved the same problems in the (reduced) frequency domain. Based on these very fundamental two-dimensional studies [26-28], the lift-deficiency functions due to a unitary step change in the angle of attack and a unitary sharp-edged vertical gust [29] have been investigated for thin flat wings of various shapes [30-38], including elliptical [39-40], rectangular [41] swept trapezoidal [42] and delta wings [43], for which panel-based methods are particularly useful [44-47]. Alternatively, the aerodynamic indicial functions have empirically been obtained by collecting data from dedicated wind tunnel tests [48-53].

More recently, computational fluid dynamics (CFD) [54] has also been employed as the most general high-fidelity aerodynamic tool [55-58], capable of calculating numerically the unsteady load build-up of arbitrary wings in any (practical) flow condition [59-61]. However, CFD simulations are still computationally expensive and rather sensitive to the specific model settings; they often require a significant amount of pre- and post- processing efforts as well as specialist experience to prevent numerical instability and grid singularity [62] (which is a prerequisite for robust and reliable implementations of fully-automatic parametrised MDO routines) and thus grant correct convergence to physically and mathematically sound results, to be confirmed by either rigorous analytical validation or trusted experimental evidence [63]. Indeed, coupling CFD with complex structural solvers [64-65] is still a challenge [66-67].

In order to re-write the aerodynamic load build-up in the state-space form [68-69] suitable for aero-servo-elastic simulations, nonlinear optimisation [70-71] has then been used to obtain the best analytical approximation for the indicial functions as a series of exponential/rational functions with optimal time-constants/poles and amplitudes/gains in the (reduced) time/frequency domain [72-77]; the optimal curve fitting [78] was historically performed in both domains, which are related via Laplace transform [79-80]. Due to fluid dynamics similitude [81], the approximate lift-deficiency functions may finally be parametrised with respect to few fundamental nondimensional numbers, such as Reynolds, Mach and Strouhal numbers of the airflow [82] as well as sweep angle, aspect and thickness ratios of the aircraft wing [42]; correction-based approaches have also been proposed in order to retain the high accuracy of nonlinear CFD at the low computational costs of linear potential-flow aerodynamics [83-86].

In this paper, the lift-deficiency coefficients due to a unitary step change in the angle of attack and a unitary sharp-edged vertical gust are first obtained in the (reduced) time domain for both elliptical and rectangular thin wings of arbitrary aspect ratio, by means of different semi-analytical reduced-order models developed from previous works in the literature [39,42].

Nonlinear optimisation [70] is then employed to find their best approximation as a series of exponential functions with optimal time constants and amplitudes [17,75], where the root mean squared error (RMSE) is set as the objective function to be minimised and the maximum absolute error (MAXE) is monitored [87]. Depending on the availability of the lift-deficiency coefficient, the optimal curve fitting [78] is performed in either the (reduced) time or the (reduced) frequency domain, where the optimal approximation parameters act as the constrained optimisation variables and sequential quadratic programming (SQP) [88-89] is employed as the optimisation algorithm. The optimal coefficients of the approximate lift-deficiency functions are finally tabulated and analytically expressed as function of the wing's aspect ratio, for each type of wing and flow perturbation. The obtained parametric reduced-order models are hence critically discussed and their mathematical features clarified in terms of their main physical assumptions, so to provide with the best theoretical insight.

2 ELLIPTICAL WINGS

Flat elliptical wings (x, y) are geometrically defined as [39]:

$$x = \frac{c_R}{2}\sin\theta\,, \qquad y = \frac{b}{2}\cos\theta\,, \tag{1}$$

where c_R is the root chord, b the span and θ the polar angle; thus, their local chord $c(y)$, surface S and aspect ratio AR are explicitly given by:

$$c = c_R\sqrt{1-\left(\frac{2y}{b}\right)^2}\,, \qquad S = \frac{\pi}{4}bc_R\,, \qquad AR = \frac{4b}{\pi c_R}\,. \tag{2}$$

For such wings, the influence of the tip vortices on the lift distribution along the span may be calculated based on lifting line theory as function of the aspect ratio (which introduces the dependency of the airload on the finite wing span [81,90]) and the unsteady lift of the three-dimensional wing hence obtained from the one of the two-dimensional airfoil [91-92]. In particular, considering a suitable distribution of elementary vortex loops, the lift-deficiency coefficient $C_L^{3D}(t)$ of the wing may be calculated in the (reduced) time domain as [39]:

$$C_L^{3D} = (1-w_{i0})C_L^{2D} - \int_0^\tau \frac{dw_i(\xi)}{d\xi}C_L^{2D}(\tau-\xi)d\xi\,, \qquad \tau = \frac{2V_\infty}{c_R}t\,, \tag{3}$$

where τ and t are the reduced and physical time, respectively, whereas V_∞ is the reference flow speed, $C_L^{2D}(t)$ is the airfoil's lift-deficiency coefficient, $\Gamma_w^{3D}(t)$ the related circulation and $w_i(t)$ the induced wing downwash, which evolve as [39]:

$$\Gamma_w^{3D} = (1-w_{i0})\Gamma_w^{2D} - \int_0^\tau \frac{dw_i(\xi)}{d\xi}\Gamma_w^{2D}(\tau-\xi)d\xi\,, \tag{4}$$

$$w_i = w_\Gamma \Gamma_{w0}^{3D} + \int_0^\tau \frac{d\Gamma_w^{3D}(\xi)}{d\xi} w_\Gamma(\tau - \xi) d\xi \,,$$

with $\Gamma_w^{2D}(t)$ the airfoil circulation induced by a unitary step in the wing downwash and $w_\Gamma(t)$ the wing downwash induced by a unitary step in the wing circulation.

The airfoil's lift coefficient and circulation may be calculated using Peters' inflow theory [91-92] and reciprocity relations [93-95] for thin airfoils and then analytically approximated as a series of n exponential terms as [96]:

$$\begin{aligned} C_L^{2D} &= 2\pi\left(1 - \sum_{j=1}^{n^C} A_j^C e^{-B_j^C \tau}\right), \qquad & \sum_{j=1}^{n^C} A_j^C &= 1 - \frac{C_{L0}^{2D}}{2\pi}, \\ \Gamma_w^{2D} &= 2\pi\left(1 - \sum_{j=1}^{n^\Gamma} A_j^\Gamma e^{-B_j^\Gamma \tau}\right), \qquad & \sum_{j=1}^{n^\Gamma} A_j^\Gamma &= 1, \end{aligned} \tag{5}$$

where all coefficients A_j^C, B_j^C and A_j^Γ, B_j^Γ may be obtained by fitting the exact curves [20-25], as the result of a nonlinear constrained optimisation problem [70] where the approximation error is minimised in a root mean square sense [96] (see Appendix A). Note that the exact asymptotic (steady) conditions $C_{L\infty}^{2D} = 2\pi$ and $\Gamma_{w\infty}^{2D} = 2\pi$ are indeed automatically satisfied and this is also true for the exact initial conditions [91-92], being $C_{L0}^{2D} = \pi$ in the case of Wagner's function for the unsteady lift due to a unitary step change in the angle of attack and $C_{L0}^{2D} = 0$ in the case of Kussner's function for the unsteady lift due to a unitary sharp-edge gust, with $\Gamma_{w0}^{2D} = 0$ in both cases. It is important to stress that Kussner's lift-deficiency function is also the airfoil circulation corresponding to Wagner's lift-deficiency function [93-95].

The wing downwash may be calculated as the vertical velocity induced at the mid-chord by a vortex ring extending along the wake and reads [39]:

$$w_\Gamma = \frac{1}{\pi b}\left\{\frac{2x_w}{b} sK + \frac{b}{2x_w}\left[\left(s - \frac{1}{s}\right)K + \frac{E}{s} - 1\right]\right\}, \qquad s = \left[1 + \left(\frac{2x_w}{b}\right)^2\right]^{-\frac{1}{2}}, \tag{6}$$

where $K(s)$ and $E(s)$ are the elliptic integrals of the first and second kinds [97], respectively, which are functions of the nondimensional spatial variable s, with $x_w = V_\infty t$ the wake length behind the mid-chord; since $s = 1$, $K = \infty$ and $E = 1$ for $t = 0$, the wing downwash is initially $w_{\Gamma 0} = 0$ and then reaches the asymptotic steady condition $w_{\Gamma\infty} = \frac{1}{2b}$, as $s = 0$, $K = \frac{\pi}{2}$ and $E = \frac{\pi}{2}$ for $t = \infty$. In fact, by conveniently fixing $c_R = 2$, with $b = \frac{\pi AR}{2}$ and $x_w = \tau$, the wing downwash can more suitably be rewritten in terms of both wing aspect ratio and reduced time (i.e., the number of travelled semi-chords) as:

$$w_\Gamma = \frac{2}{\pi^2 AR}\left\{\frac{4\tau}{\pi AR}sK + \frac{\pi AR}{4\tau}\left[\left(s-\frac{1}{s}\right)K + \frac{E}{s} - 1\right]\right\}, \qquad s = \left[1+\left(\frac{4\tau}{\pi AR}\right)^2\right]^{-\frac{1}{2}}, \tag{7}$$

and then also analytically approximated as a series of n exponential terms as:

$$w_\Gamma = \frac{1}{\pi AR}\left(1 - \sum_{j=1}^{n^w} A_j^w e^{-B_j^w \frac{\tau}{AR}}\right), \qquad \sum_{j=1}^{n^w} A_j^w = 1, \tag{8}$$

where all coefficients A_j^w and B_j^w may still be obtained by fitting the exact curve and both initial $w_{\Gamma 0} = 0$ and asymptotic $w_{\Gamma\infty} = \frac{1}{\pi AR}$ exact conditions are automatically satisfied. However, as the wing wake actually leaves from the trailing edge, the initial length x_{w0} of the wing wake is set equal to half of the wing's mean geometric chord $\bar{c} = \frac{\pi c_R}{4}$ [39] and the wing downwash may finally be written as:

$$w_\Gamma = \frac{1}{\pi AR}\left(1 - \sum_{j=1}^{n^w} A_j^w e^{-B_j^w \frac{(\tau-\tau_0)}{AR}}\right), \qquad \tau_0 = -\frac{\pi}{4}. \tag{9}$$

Integrating by parts, the three-dimensional lift-deficiency coefficient, related wing circulation and induced wing downwash can conveniently be rewritten as [96]:

$$\begin{aligned} C_L^{3D} &= C_L^{2D} - w_i C_{L0}^{2D} + \int_0^\tau \frac{dC_L^{2D}(\tau-\xi)}{d\xi} w_i(\xi) d\xi, \\ \Gamma_w^{3D} &= \Gamma_w^{2D} - w_i \Gamma_{w0}^{2D} + \int_0^\tau \frac{d\Gamma_w^{2D}(\tau-\xi)}{d\xi} w_i(\xi) d\xi, \\ w_i &= \Gamma_w^{3D} w_{\Gamma 0} - \int_0^\tau \frac{dw_\Gamma(\tau-\xi)}{d\xi} \Gamma_w^{3D}(\xi) d\xi; \end{aligned} \tag{10}$$

due to Laplace transformation [79-80], the integral convolution process in the (reduced) time domain can then be realised by the equivalent differential form:

$$\begin{aligned} C_L^{3D} &= C_L^{2D} - w_i C_{L0}^{2D} - 2\pi \sum_{j=1}^{n^C} A_j^C z_j^C, \\ \Gamma_w^{3D} &= \Gamma_w^{2D} - w_i \Gamma_{w0}^{2D} - 2\pi \sum_{j=1}^{n^\Gamma} A_j^\Gamma z_j^\Gamma, \\ w_i &= \Gamma_w^{3D} w_{\Gamma 0} + \frac{1}{\pi AR} \sum_{j=1}^{n^w} A_j^w e^{-\frac{\pi B_j^w}{4AR}} z_j^w, \end{aligned} \tag{11}$$

where the added aerodynamic states $z(t)$ are defined in the (reduced) Laplace domain p as:

$$z_j^C = \frac{B_j^C w_i}{p + B_j^C}, \qquad z_j^\Gamma = \frac{B_j^\Gamma w_i}{p + B_j^\Gamma}, \qquad z_j^w = \frac{B_j^w \Gamma_w^{3D}}{p + B_j^w}, \tag{12}$$

and evolve in the (reduced) time domain as [96]:

$$\frac{dz_j^C}{d\tau} + B_j^C z_j^C = B_j^C w_i, \qquad \frac{dz_j^\Gamma}{d\tau} + B_j^\Gamma z_j^\Gamma = B_j^\Gamma w_i, \qquad \frac{dz_j^w}{d\tau} + B_j^w z_j^w = B_j^w \Gamma_w^{3D}, \tag{13}$$

with initial conditions $z_j^{C0} = 0$, $z_j^{\Gamma 0} = 0$ and $z_j^{w0} = 0$. The resulting asymptotic conditions are $C_{L\infty}^{3D} = \frac{2\pi AR}{2 + AR}$, $\Gamma_{w\infty}^{3D} = \frac{2\pi AR}{2 + AR}$ and $w_{i\infty} = \frac{2}{2 + AR}$, in perfect agreement with lifting line theory for elliptical wings [90]; therefore, the computed wing's lift-deficiency coefficient may analytically be approximated as a series of n exponential terms as:

$$C_L^{3D} = \frac{2\pi AR}{2 + AR}\left(1 - \sum_{j=1}^{n} A_j e^{-B_j \tau}\right), \qquad \sum_{j=1}^{n} A_j = 1 - \frac{C_{L0}^{3D}}{2\pi}\left(1 + \frac{2}{AR}\right), \tag{14}$$

where all coefficients A_j and B_j are consistently obtained by fitting the numerically integrated curve for each aspect ratio and both asymptotic and initial exact conditions are automatically satisfied, being $C_{L0}^{3D} = \pi$ in the case of a unitary step change in the angle of attack and $C_{L0}^{3D} = 0$ in the case of a unitary sharp-edge gust, with $\Gamma_{w0}^{3D} = 0$ and $w_{i0} = 0$ in both cases. Note that both Wagner's [20] and Kussner's [21-22] functions are correctly obtained in the limit of infinite wing.

In fact, due to the Kutta-Joukowsky condition [98-99], the impulsive start of the wing wake (which initially moves as an extension of the wing) generates some flow inertia which modifies the initial behaviour of the load build-up, especially for a unitary step change in the angle of attack. This further three-dimensional effect may be calculated by considering the two-dimensional distribution of kinetic potential $\Phi(t)$ and pressure difference $\Delta p(t)$ over each wing section in normal motion, namely [39]:

$$\Phi = \frac{w}{E}\sqrt{(1 + x)(1 - x + \tau)}, \qquad \Delta p = -2\rho_\infty V_\infty \left(\frac{\partial \Phi}{\partial \tau} + \frac{\partial \Phi}{\partial x}\right), \tag{15}$$

where ρ_∞ is the reference flow density and the variations in the kinetic potential are due to the apparent variation of the wing shape (although the change in the wing perimeter may be neglected during widening). In particular, with $x = \cos\theta$, right at the wake start it is [39]:

$$\Phi_0 = \frac{w}{E}\sin\theta, \qquad \Delta p_0 = \rho_\infty V_\infty \frac{w(\cos\theta - 1)}{E \sin\theta}, \qquad C_{L0}^{3D} = \int_{-1}^{+1} \frac{\Delta p_0 dx}{\rho_\infty V_\infty^2}, \tag{16}$$

where $w = V_\infty$ for a unitary angle of attack; therefore, the approximate initial behavior of the wing's lift-deficiency coefficient may then be estimated by suitably scaling the approximate initial behavior of the airfoil's lift-deficiency coefficient [93] as (see Appendix B):

$$\lim_{\tau\to 0} C_L^{3D} \approx \frac{\pi}{E}\left(1+\frac{\tau}{4}\right), \qquad \lim_{\tau\to 0} C_L^{3D} \approx \frac{2}{E}\sqrt{2\tau}\,, \tag{17}$$

for the case of unitary step change in the angle of attack and unitary sharp-edge gust, respectively. Note that, due to the gust penetration effect, this three-dimensional correction may reasonably be neglected in the latter case [39], since the initial perturbations of both kinetic potential and tip-vortices strength are fairly marginal, the wing's lift-deficiency coefficient starting at zero directly and then increasing very rapidly with an infinite theoretical rate. Thus, by accounting for the flow inertia acting at the impulsive start of the wake, the wing's lift-deficiency coefficient due to a unitary step change in the angle of attack can finally be approximated as:

$$C_L^{3D} = \frac{2\pi AR}{2+AR}\left(1-\sum_{j=1}^{n+1} A_j e^{-B_j\tau}\right), \qquad \sum_{j=1}^{n} A_j = 1-\frac{2+AR}{2AR}, \tag{18}$$

where the two coefficients of the additional exponential term read:

$$A_{n+1} = \frac{2+AR}{2AR}\left(1-\frac{1}{E}\right), \qquad B_{n+1} = \frac{1}{A_{n+1}}\left(\frac{2+AR}{8EAR}-\sum_{j=1}^{n} A_j B_j\right), \tag{19}$$

and Wagner's function [20] is still correctly obtained in the limit of infinite wing.

3 TRAPEZOIDAL WINGS

Flat trapezoidal wings the local chord is explicitly given by [42]:

$$c = c_R\left[1-2(1-\lambda)\frac{y}{b}\right], \qquad \lambda = \frac{c_T}{c_R}\,, \tag{20}$$

where $0 \le \lambda \le 1$ is the taper ratio and c_T the tip chord; surface and aspect ratio then read:

$$S = \left(\frac{1+\lambda}{2}\right) b c_R\,, \qquad AR = \left(\frac{2}{1+\lambda}\right)\frac{b}{c_R}\,, \tag{21}$$

respectively, for any sweep angle Λ. The latter is geometrically defined with respect to the wing's quarter chord line, where the aerodynamic centre of each wing section is assumed in accordance with thin airfoil theory [100]; the downwash control point is then consistently located at the three-quarter chord, where the non-penetration boundary condition for inviscid potential flow is satisfied [47]. In particular, fully symmetrical wings with isosceles trapezoidal planform own $\tan\Lambda = \frac{1}{AR}\left(\frac{1-\lambda}{1+\lambda}\right)$, which gives $\tan\Lambda = \frac{1}{AR}$ for isosceles triangular

wings (with straight symmetry axis); whereas forward and backward swept wings with trapezoidal planform own $\tan\Lambda=\frac{1}{AR}\left(\frac{\lambda-1}{1+\lambda}\right)$ and $\tan\Lambda=\frac{3}{AR}\left(\frac{1-\lambda}{1+\lambda}\right)$, which give $\tan\Lambda=-\frac{1}{AR}$ and $\tan\Lambda=\frac{3}{AR}$ for forward and backward delta wings (with straight leading and trailing edge), respectively; in all cases, a straight wing characterised by two-dimensional flow is correctly obtained in the limit of infinite wing. Rectangular and parallelogram wings have $\lambda=1$, while rhomboidal and delta wings have $\lambda=0$.

Within a simplified yet effective approach [42], a single vortex-ring is considered for modeling the total (lumped) wing circulation and a single control point is then placed at the third quarter of the wing's root chord. Both bound and shed vortex lines are parallel to the wing's quarter chord line, whereas the two wing-tip trailed vortex lines are parallel to the free-stream. All vortices have the same (lumped) intensity and the shed vorticity travels towards infinity with half the reference airflow speed from half the wing's root chord behind the control point, hence stretching the vortex-ring and increasing the wake length; when the wing wake eventually approaches infinity, its influence on the wing flow fades away and the steady condition is asymptotically obtained. The influence of the wing's tip vortices and wake on the (uniform yet time-varying) lift distribution along the span is then calculated with the simplest implementation of the unsteady lifting line theory [47,101-103] and the lift build-up of the three-dimensional wing is hence obtained as function of its aspect ratio, taper ratio and sweep angle. In particular, the lift-deficiency coefficient due to a unitary step change in the angle of attack was calculated in the (reduced) time domain based on Kutta-Joukowsky theorem as [42]:

$$C_L^{3D}=\frac{2\pi AR_e}{b\left(P+Q+R\right)},\qquad AR_e=\left(\frac{1+\lambda}{2}\right)AR, \tag{22}$$

where $P(t)$, $Q(t)$ and $R(t)$ give the vortex-ring contributions due to bound, wing-tip trailed and wake shed vortices, respectively, based on Biot-Savart law [47] and read [42]:

$$\begin{aligned}
bP&=AR_e\left[\frac{AR_e\sec^2\Lambda-\tan\Lambda}{\sqrt{\left(AR_e\sec\Lambda-\sin\Lambda\right)^2+\cos^2\Lambda}}+\tan\Lambda\right],\\
bQ&=\frac{1-AR_e\tan\Lambda}{\sqrt{\left(1-AR_e\tan\Lambda\right)^2+AR_e^2}}+\frac{1+AR_e\tan\Lambda+\frac{\tau}{2}}{\sqrt{\left(1+AR_e\tan\Lambda+\frac{\tau}{2}\right)^2+AR_e^2}},\\
bR&=\frac{AR_e}{1+\frac{\tau}{2}}\left\{\frac{AR_e\sec^2\Lambda+\left(1+\frac{\tau}{2}\right)\tan\Lambda}{\sqrt{\left[AR_e\sec\Lambda+\left(1+\frac{\tau}{2}\right)\sin\Lambda\right]^2+\left[\left(1+\frac{\tau}{2}\right)\cos\Lambda\right]^2}}-\tan\Lambda\right\};
\end{aligned} \tag{23}$$

the wing's lift-deficiency coefficient may finally be approximated as a series of n exponential terms as:

$$C_L^{3D} = C_{L\infty}^{3D}\left(1-\sum_{j=1}^{n} A_j e^{-B_j\tau}\right), \qquad \sum_{j=1}^{n} A_j = 1-\frac{C_{L0}^{3D}}{C_{L\infty}^{3D}}, \tag{24}$$

where all coefficients A_j and B_j are obtained by fitting the exact analytical curve [42] and both asymptotic and initial exact conditions are automatically satisfied.

For the special case of rectangular wing, $\lambda = 1$ and $\Lambda = 0$ and the lift-deficiency coefficient reduces to:

$$C_L^{3D} = \frac{2\pi AR}{\sqrt{1+AR^2}+\dfrac{2}{2+\tau}\sqrt{\left(1+\dfrac{\tau}{2}\right)^2+AR^2}}, \tag{25}$$

with initial behavior and asymptotic (steady) condition given by:

$$\lim_{\tau\to 0} C_L^{3D} \approx \frac{\pi AR}{\sqrt{1+AR^2}}\left[1+\left(\frac{AR^2}{1+AR^2}\right)\frac{\tau}{4}\right], \qquad C_{L\infty}^{3D} = \frac{2\pi AR}{1+\sqrt{1+AR^2}}, \tag{26}$$

respectively, which degenerates into Garrick's approximation [93] of Wagner's function for thin airfoils in the limit of infinite wing. Note that, due to the intrinsic limitations of the simple vortex-system representation employed, it is known that the calculated asymptotic (steady) conditions are not very accurate and should rather be provided by other higher-fidelity sources (e.g., lifting line theory [90] as in Appendix B, vortex or doublet lattice methods [104], computational fluid dynamics [54], wind tunnel tests [51]). In any case, the reported model [42] is better suited for slender thin wings with high aspect and taper ratios as well as small sweep angle, for which the three-dimensional flow and geometry effects are less significant (i.e., the induced downwash speed is smaller and the control points of each wing section are closer to the one at the root section).

Unfortunately, no analytical expression was provided for the lift-deficiency function due to a unitary sharp-edge gust [42]. Nevertheless, this may numerically be obtained in the (reduced) frequency domain by multiplying the Laplace transform of the lift-deficiency function due to a unitary step change in the angle of attack by the transfer function of the gust penetration effect, which is here approximated as the ratio between (modified) Sears' and Theodorsen's functions [23-25] (see Appendix A); the corresponding lift-deficiency function in the (reduced) time domain may then be obtained via inverse Laplace transform [79-80]. Note that this is equivalent to convolving the lift-deficiency function due to a unitary step change in the angle of attack with the delay function given by the inverse Laplace transform of the transfer function of the gust penetration effect [96]. Of course, it is implicitly assumed that all wing sections encounter the wind gust at the same time, even in the case of swept tapered wings [42].

4 NONLINEAR CONSTRAINED OPTIMIZATION FOR BEST APPROXIMATION

The lift-deficiency functions due to a unitary step change in the angle of attack and unitary sharp-edge gust for elliptical wings [39], as well as those due to a unitary step change in the angle of attack for rectangular wings [42], were either numerically obtained or analytically expressed in the (reduced) time domain directly, where their best approximation as a series of

exponential terms with optimal time constants and amplitudes is sought [96]. On the contrary, the lift-deficiency functions due to a unitary sharp-edge wind gust for rectangular wings were numerically obtained in the (reduced) frequency domain, where their best approximation as a series of rational terms with optimal poles and gains is sought [96]; the corresponding best approximation of the lift-deficiency function as a series of exponential functions in the (reduced) time domain is then obtained via inverse Laplace transform [79-80].

Analytical approximation functions with many free coefficients may generally better adapt to the target curve and reproduce its local features but also misbehave between sample points, especially when just few spare are available [78]. An adequate selection of the sample points is hence necessary [105], since their "fixity" drives the "flexibility" of the analytical function, and, in order to avoid focusing on certain regions of the lift-deficiency functions a priori, a uniform distribution of $N=100$ sample points is here first obtained by imposing an equal distance among each couple of consecutive sample points and solving a preliminary nonlinear optimisation problem [96]. Then, with $F(\chi)$ the target curve, the quality of its analytical approximation $\widetilde{F}(\chi)$ is assessed at the sample points χ according to the MAXE and RMSE, namely [87]:

$$\mathrm{MAXE}=\max\left|\widetilde{F}(\chi)-F(\chi)\right|, \qquad \mathrm{RMSE}=\frac{\left\|\widetilde{F}(\chi)-F(\chi)\right\|}{\sqrt{N}}, \tag{27}$$

the latter being set as the objective function to be minimised in the nonlinear optimisation problem, under the constrains given on the approximation function coefficients in order to satisfy the exact limit conditions of the lift-deficiency functions [96]. This choice of the objective function ensures the approximation function being close to the exact curve, as many sample points are indeed readily available in the present case; otherwise, a parametric aggregate objective function where the RMSE of the segments connecting consecutive sample points is also minimised is suggested, which ensures the approximation function being rather smooth without oscillating much around the exact curve [96].

SQP has been employed as gradient-based, iterative optimisation algorithm [88-89], which assumes both the objective function and the constraints are twice continuously differentiable and searches for the point where the gradient of the objective function vanishes within a general Lagrangian formulation, reducing to Newton's method for unconstrained problems [70]. The heuristic gradient-free Nelder-Mead simplex method (NMSM, where the absolute value of the poles was considered for a meaningful unconstrained implementation of the problem) [106] and genetic algorithm (GA, where the initial population was taken as the SQP solution in order to boost convergence) [107] were also employed and the same optimal results eventually obtained, confirming the consistency and robustness of the proposed approach as well as granting confidence the global optimum was actually reached in all cases.

5 LIFT-DEFICIENCY FUNCTIONS AND THEIR OPTIMAL APPROXIMATION

Considering a flat elliptical wing with $AR=3$ and $AR=6$, Jones' preliminary results for the three-dimensional lift-deficiency coefficient due to a unitary step change in the angle of attack [39] are reproduced in Figure 1 (left) for code validation purposes. These results are based on Jones' analytical exponential approximations shown in Figure 1 (right) for the wing downwash build-up as well as Figure 2 for the lift-deficiency coefficient and related circulation due to a unitary step change in the angle of attack of a two-dimensional flat plate. The

proposed analytical approximations (see Appendix A) are also shown in the same figures for direct comparison, along with the exact curves wherever available; the approximations coefficients are summarised in Table 1.

Apart from the initial correction due to the impulsive start of the wing wake [39], Jones's draft results depart from the final ones where his approximations of both wing downwash and especially airfoil circulation depart from the respective exact curves, without approaching the correct asymptotic value and hence artificially increasing the wing's lift coefficient; it is then apparent that accurate analytical approximations are strictly necessary for all flow variables.

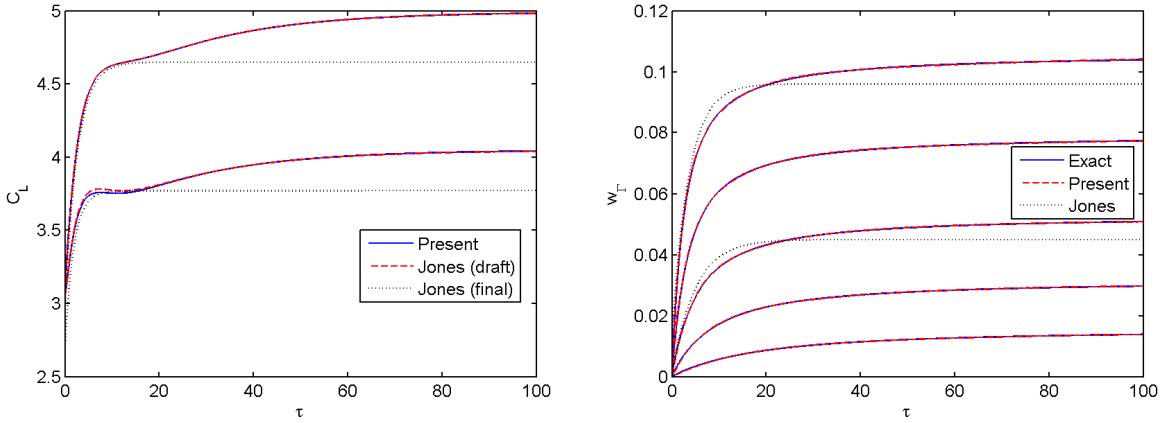

Figure 1. Lift-deficiency coefficient (left) and wing downwash (right) due to a unitary step change in the angle of attack for flat elliptical wing with AR=3,6 (left) and AR=3,4,6,10,20 (right)

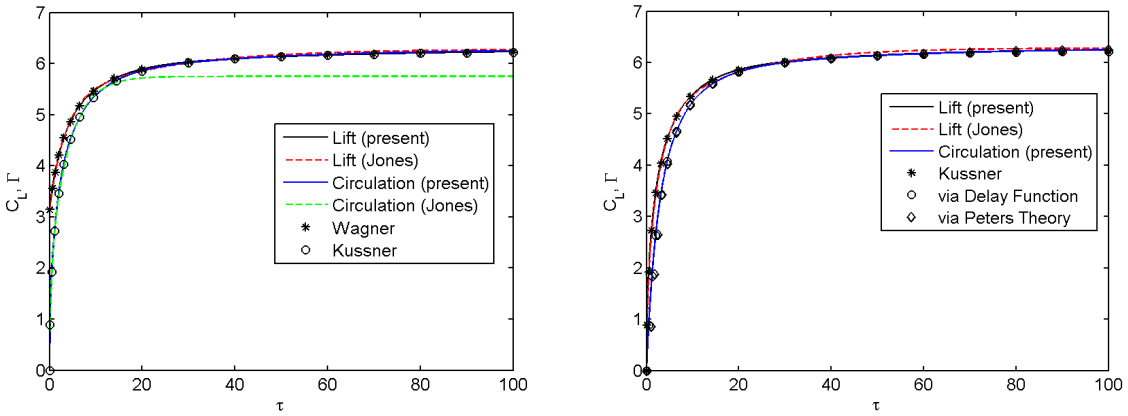

Figure 2. Lift-deficiency function and circulation due to a unitary step change in the angle of attack (left) and unitary sharp-edge gust (right) for flat airfoil

Table 1. Coefficients of the exponential approximation for the fundamental flow variables

	A_1	A_2	A_3	A_4	A_5	B_1	B_2	B_3	B_4	B_5
$C_{L\alpha}^{2D}$	0.0684	0.2657	0.1659	-	-	0.0222	0.1343	0.4915	-	-
C_{Lg}^{2D}	0.0954	0.3836	0.3184	0.1380	0.0646	0.0291	0.1673	0.6602	4.2399	69.585
Γ_{wg}^{2D}	0.0973	0.4522	0.4382	0.0123	-	0.0287	0.1602	0.5011	2.2338	-
w_Γ	0.0924	0.3730	0.5346	-	-	0.0483	0.3788	1.5867	-	-

Figure 3 shows the lift-deficiency coefficient due to a unitary step change in the angle of attack and a unitary sharp-edge gust for elliptical wings with different aspect ratios; the optimal approximation is also shown and the relative coefficients are presented in Table 2, for the case $n = 2$. Indeed, two exponential terms appear sufficient to grant a good approximation; however, an additional one is still needed for reproducing the correct initial behavior of the three-dimensional lift development due to a unitary step change in the angle of attack [39] and would be beneficial to improve the accuracy of the three-dimensional lift development due to a unitary sharp-edge gust [96]. Figures 4 and 5 then show the analytical approximation of these coefficients as function of the inverse of the wing's aspect ratio, as implicitly suggested by the generalised formula for the wing downwash. In particular, a cubic polynomial is generally found sufficient and exhibits a linear behavior for high (inverse) aspect ratios, where all approximation coefficients converge to the ones characterising two-dimensional flow (i.e., the intercepts). Note that Jones' results [39] are rather conservative, as they provide the wing with a faster load build-up and the asymptotic (steady) conditions reached much earlier; this is mainly due to the approximations of both airfoil circulation and wing downwash being conservative in the first place and just a single exponential term being adopted (see Appendix B).

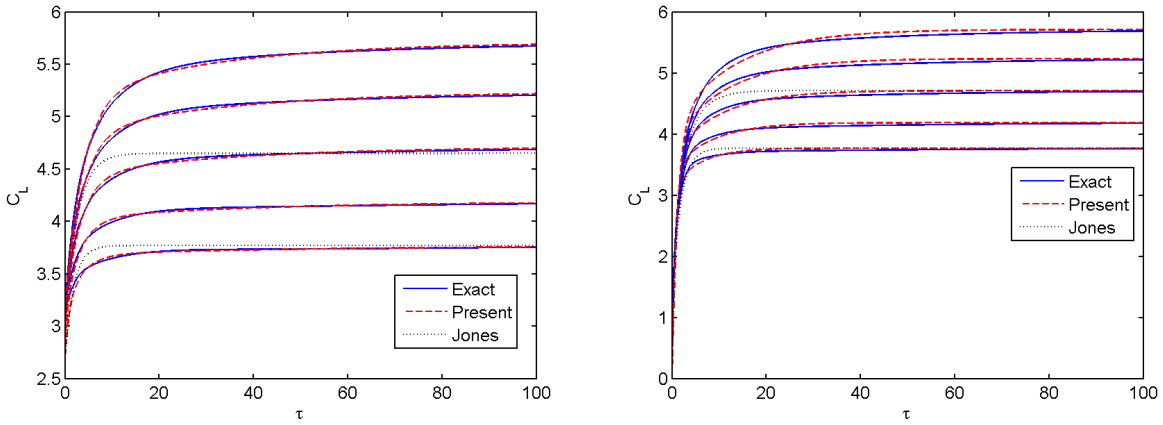

Figure 3. Lift-deficiency coefficient due to a unitary step change in the angle of attack (left) and a unitary sharp-edge gust (right) for flat elliptical wing with AR=3,4,6,10,20

Table 2. Coefficients of the exponential approximation for the lift-deficiency functions of an elliptical wing

	angle of attack				***sharp-edge gust***			
AR	A_1	A_2	B_1	B_2	A_1	A_2	B_1	B_2
3	0.0235	0.1432	0.0190	0.2954	0.1736	0.8264	0.1729	1.5882
4	0.0398	0.2102	0.0257	0.3156	0.1887	0.8113	0.1222	1.3119
6	0.0599	0.2734	0.0297	0.3044	0.2240	0.7760	0.0996	1.1014
10	0.0793	0.3207	0.0315	0.2842	0.2556	0.7444	0.0858	0.9421
20	0.0962	0.3538	0.0320	0.2652	0.2806	0.7194	0.0767	0.8263

Figure 6 shows the lift-deficiency coefficient due to a unitary step change in the angle of attack and a unitary sharp-edge gust for rectangular wings with different aspect ratios; the optimal approximation is also shown and the relative coefficients are presented in Table 3, for the case $n = 2$ which still grants good approximation. Note that the asymptotic (steady) lift-deficiency coefficient for rectangular wing is slightly higher than the corresponding one for elliptical wing since not very accurate [42]; in fact, it should be lower according to lifting line theory [90] (see Appendix B).

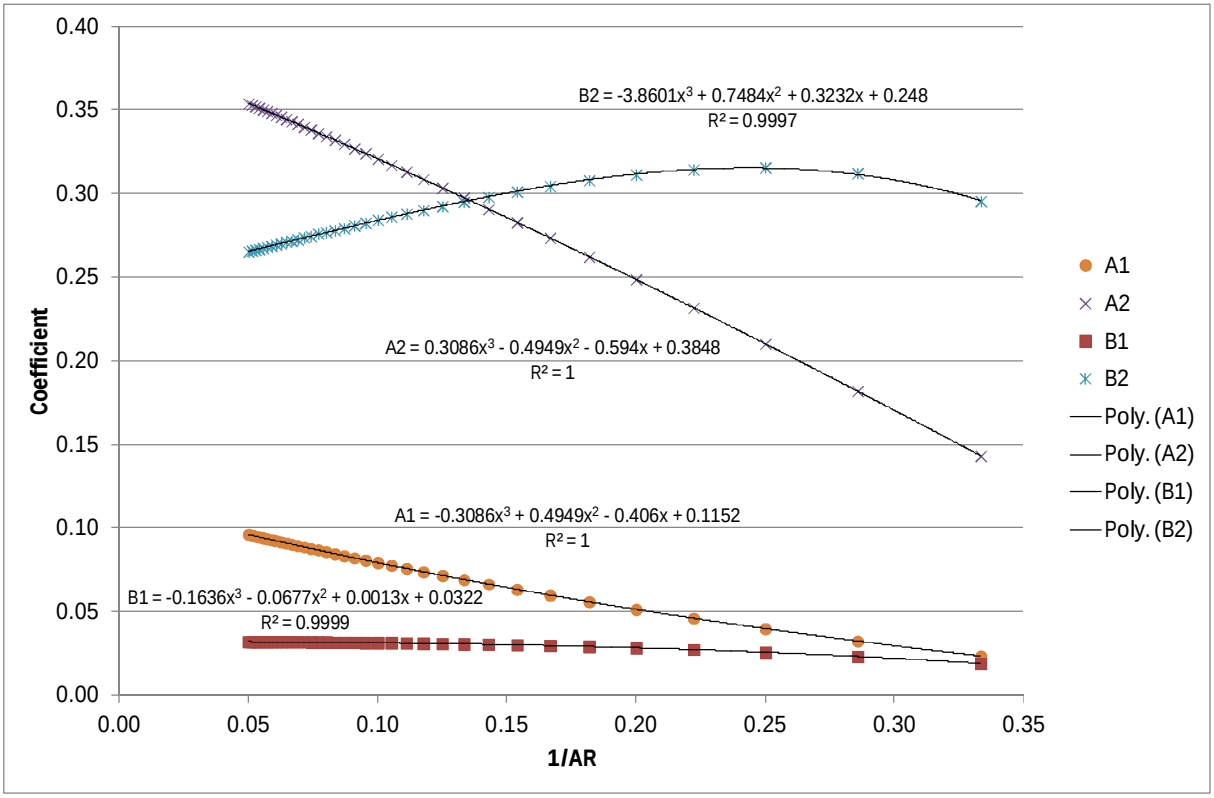

Figure 4. Coefficients of the exponential approximation for the lift-deficiency function due to a unitary step change in the angle of attack for a flat elliptical wing

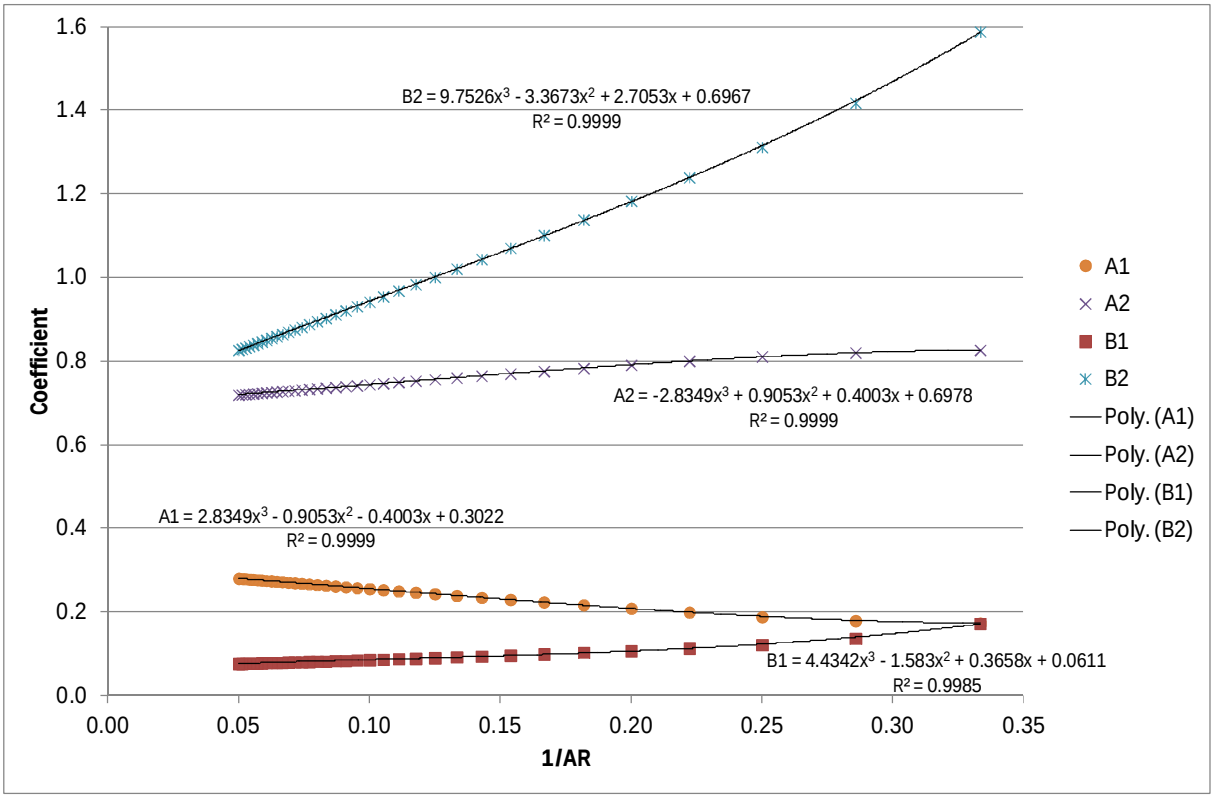

Figure 5. Coefficients of the exponential approximation for the lift-deficiency function due to a unitary sharp-edge gust for a flat elliptical wing

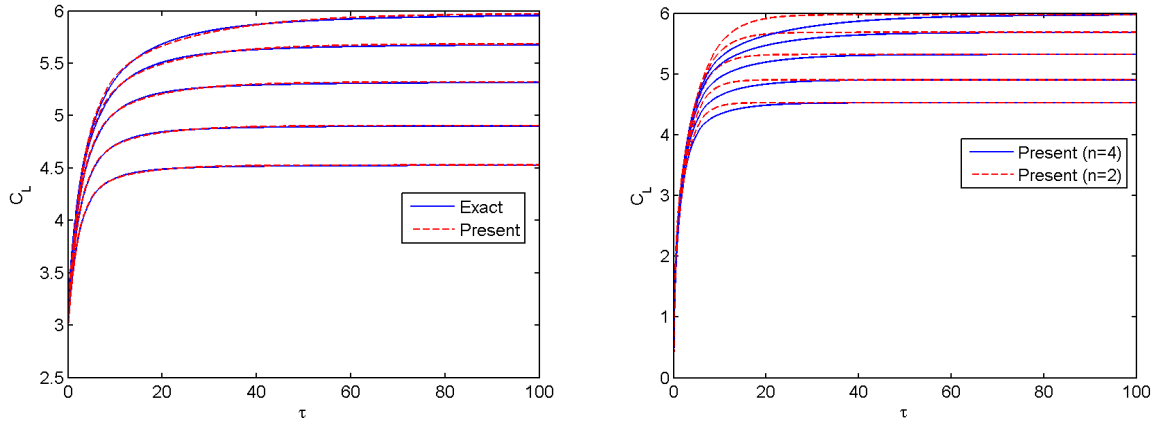

Figure 6. Lift-deficiency coefficient due to a unitary step change in the angle of attack (left) and a unitary sharp-edge gust (right) for flat rectangular wing with AR=3,4,6,10,20

Table 3. Coefficients of the exponential approximation for the lift-deficiency functions of a rectangular wing

	angle of attack				***sharp-edge gust***			
AR	A_1	A_2	B_1	B_2	A_1	A_2	B_1	B_2
3	0.0740	0.2679	0.1038	0.4781	0.6917	0.3083	0.4026	5.7145
4	0.0865	0.2923	0.0930	0.4250	0.6882	0.3118	0.3512	5.0027
6	0.1061	0.3117	0.0808	0.3741	0.6794	0.3206	0.2950	4.1989
10	0.1286	0.3216	0.0676	0.3362	0.6652	0.3348	0.2458	3.4764
20	0.1426	0.3324	0.0514	0.3041	0.6484	0.3516	0.2070	2.9203

Figure 7 shows the complex transfer function of the lift-deficiency coefficient due to a unitary sharp-edge gust for the rectangular wings with $AR = 3$ and $AR = 6$ in the (reduced) frequency domain, as numerically obtained by multiplying the Laplace transform of the lift-deficiency coefficient due to a unitary step change in the angle of attack by the delay function introducing the gust penetration effect (see Appendix A). The corresponding rational function approximations are also shown in the same figure for the cases $n = 2$ and $n = 4$, the former being rather conservative with respect to the latter, which is more accurate and hence generally suggested (note that the curve of the lift-deficiency coefficient due to a unitary sharp-edge gust should approach that of the lift-deficiency coefficient due to a unitary step change in the angle of attack from below, because of the gust penetration effect).

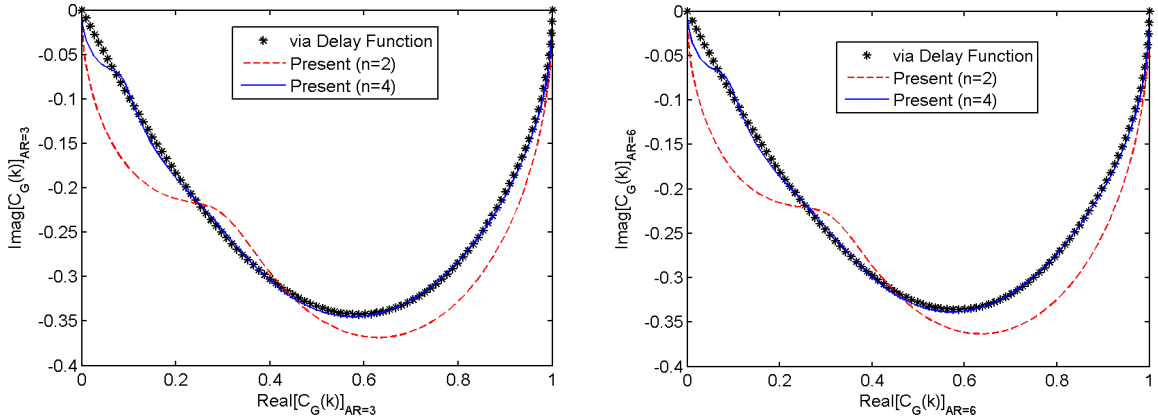

Figure 7. Lift-deficiency coefficient due to a unitary sharp-edge gust for flat rectangular wing with AR=3 (left) and AR=6 (right)

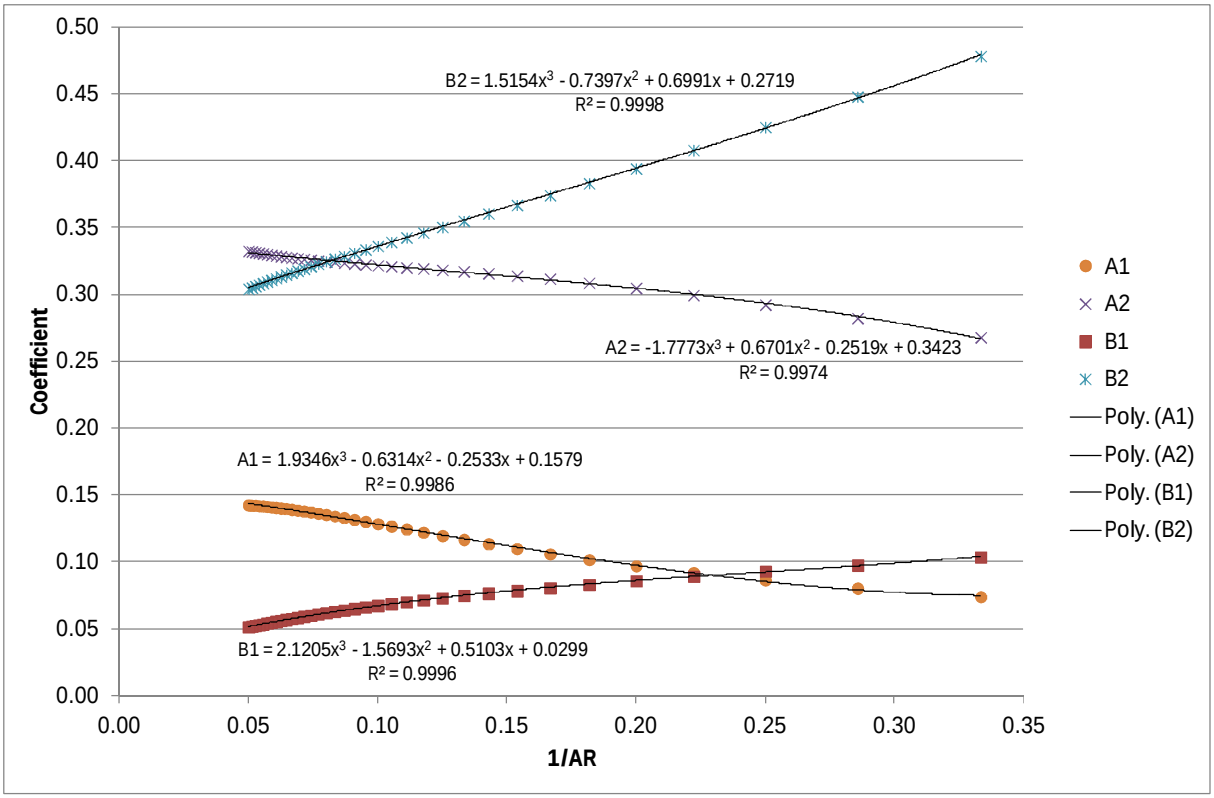

Figure 8. Coefficients of the exponential approximation for the lift-deficiency function due to a unitary step change in the angle of attack for a flat rectangular wing

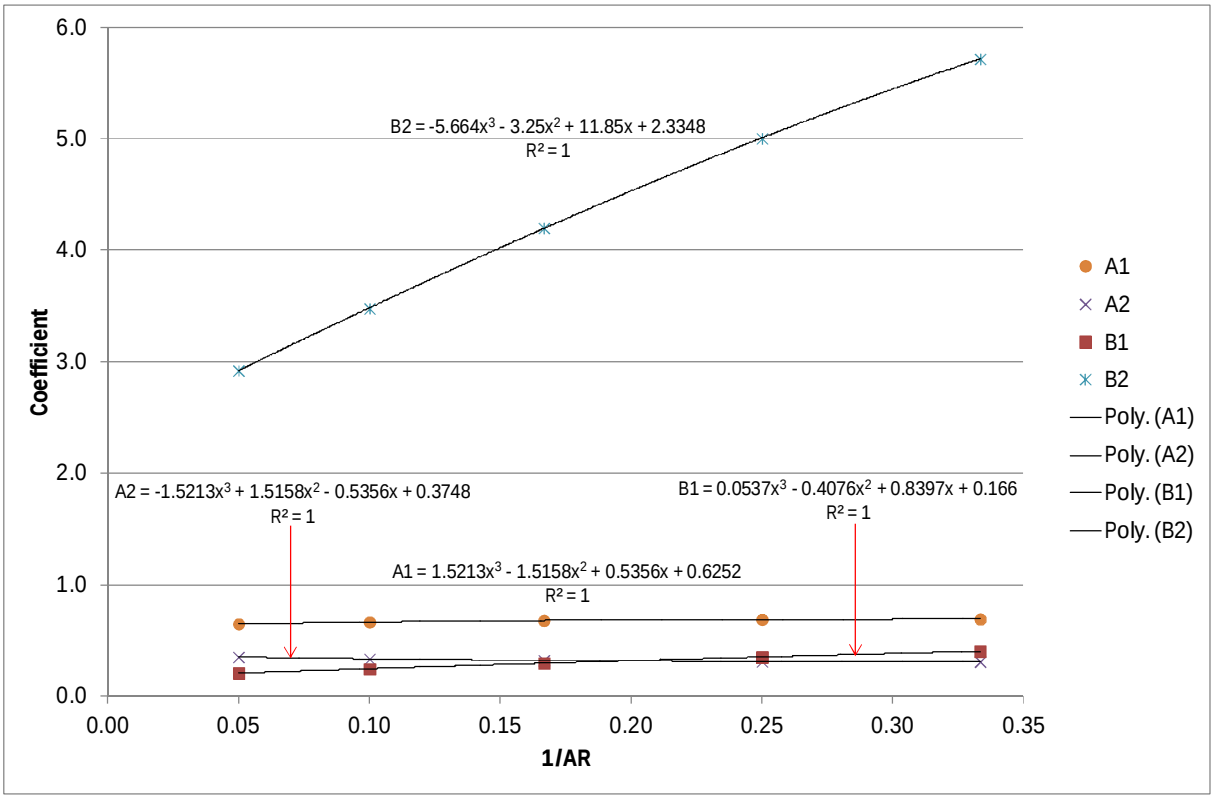

Figure 9. Coefficients of the exponential approximation for the lift-deficiency function due to a unitary sharp-edge gust for a flat rectangular wing

Figures 8 and 9 show the analytical approximation of the optimal parameters for the case $n = 2$, still as function of the inverse of the wing's aspect ratio; a cubic polynomial is again found sufficient and exhibits a linear behavior for high (inverse) aspect ratios, up to the intercept characterising two-dimensional flow. For the lift-deficiency coefficient due to a unitary step change in the angle of attack, both magnitude and trend of the approximation parameters for rectangular wing are rather similar to those for elliptical wing, as the underlying physical principles are substantially the same; for the lift-deficiency coefficient due to a unitary sharp-edge gust, higher discrepancies can be found in the magnitude of the approximation parameters, as different approaches are employed to derive the indicial function.

6 CONCLUSIONS

In this work different semi-analytical reduced-order models for calculating efficiently the unsteady aerodynamic loads of subsonic slender wings have been proposed, as intensively sought in the context of aircraft preliminary MDO. The lift-deficiency functions due to both a unitary step change in the angle of attack and a unitary sharp-edged vertical gust have first been obtained in the (reduced) time domain for both elliptical and rectangular wings of arbitrary aspect ratio, based on previous fundamental works available in the literature. Nonlinear optimisation has then been employed to find their best approximation in terms of a series of exponential functions with optimal time constants and amplitudes, allowing the load build-up to be re-written in the state-space form most suitable for aero-servo-elastic simulations and stability analyses. The approximation error being set as the objective function to be minimised, different optimisation algorithms such as SQP, NMSM and GA have been employed and provided with identical results using the least number of free parameters, thus ensuring the global optimum was reached in all cases under the prescribed constraints. Depending on the availability of the lift-deficiency function, the optimal curve fitting was performed in either the (reduced) time or the (reduced) frequency domain, which are related via Laplace transform; significant improvements were found with respect to previous approximations available in the literature, even without error-weighting. The optimal parameters have then been tabulated and finally expressed as analytical functions of the wing's aspect ratio, for each type of wing and flow perturbation. In order to offer the best theoretical insight, the obtained parametric reduced-order models have critically been assessed with respect to their mathematical features and physical assumptions and useful analogies consistently found in the results for elliptical and rectangular wings, confirming the robustness of the proposed approach. Due to their computational effectiveness, the presented semi-analytical aerodynamic models are suggested for suitable use in the preliminary MDO of flexible wings characterised by attached incompressible flow in the low-subsonic regime and may also be used to assess higher-fidelity aerodynamic tools for unsteady aerodynamics.

APPENDIX A. WAGNER, KUSSNER AND DELAY FUNCTIONS

Assuming small perturbations of incompressible potential flow, analytical solutions have been derived to calculate the unsteady airload around an oscillating flat plate in both the (reduced) time and the (reduced) frequency domains; in particular, Theodorsen [23] and Wagner [20] derived the lift-deficiency function for a unit step-change in the angle of attack, while Sears [24-25] and Kussner [21] derived the lift-deficiency function for a unit step-change in the vertical speed of a "frozen" wind gust. Due to the infinite speed propagating the perturba-

tions, circulatory and noncirculatory load contributions are distinguishable a priori [108]: given a step-change in the boundary conditions, the noncirculatory flow adapts instantaneously and embodies the flow inertia (applied at the airfoil's mid-chord), while the circulatory flow adapts with some delay and embodies the flow circulation (applied at the airfoil's aerodynamic center and control point, located at the first and last quarter-chord, respectively) [28]. Theodorsen $C(k)$ and (modified) Sears $C_G(k)$ functions being defined in the (reduced) frequency domain as [23-25]:

$$C = \frac{H_1^{(2)}}{H_1^{(2)} + \mathrm{j}H_0^{(2)}}, \qquad C_G = \left[C\left(B_0^{(1)} - \mathrm{j}B_1^{(1)}\right) + \mathrm{j}B_1^{(1)}\right]e^{-\mathrm{j}k}, \tag{A1}$$

with $H_n^{(2)}(k) = B_n^{(1)}(k) - \mathrm{j}B_n^{(2)}(k)$ Hankel functions of the second type and n-th order while $B_n^{(1)}(k)$ and $B_n^{(2)}(k)$ Bessel functions of the first and second type and n-th order, Wagner $\phi(\tau)$ and Kussner $\psi(\tau)$ functions are then defined in the (reduced) time domain as [20-21]:

$$\phi = \int_{-\infty}^{\infty} \frac{Ce^{\mathrm{j}k\tau}}{2\pi\mathrm{j}k}dk, \qquad \psi = \int_{-\infty}^{\infty} \frac{C_G e^{\mathrm{j}k\tau}}{2\pi\mathrm{j}k}dk, \tag{A2}$$

and quantify the decaying influence of the wake's inflow speed on the airfoil lift, in terms of semi-chords travelled by the shed vorticity [28].

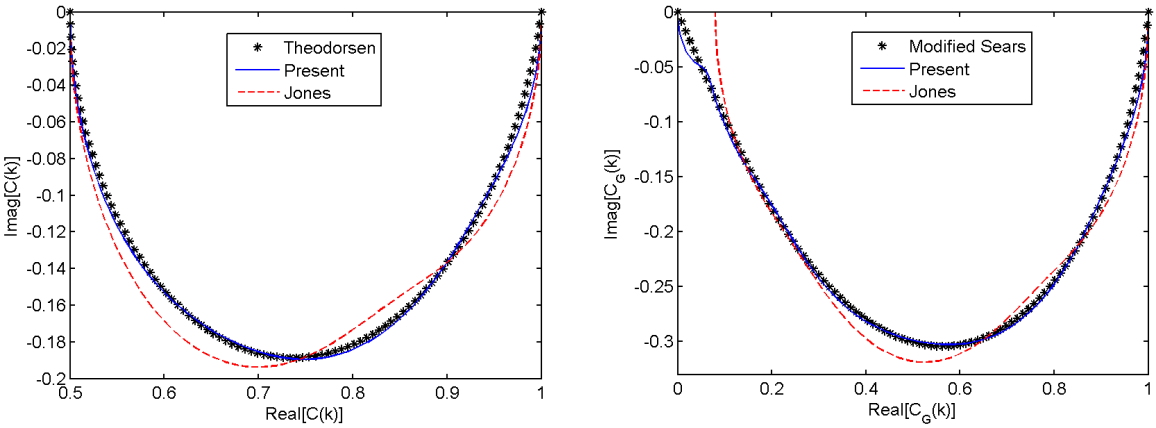

Figure A1. Theodorsen (left) and modified Sears (right) functions and their approximations

Figure A1 shows both Theodorsen and modified Sears functions along with their optimal analytical approximations; the initial guess for the optimal parameters was taken from those found in the literature [39]; deviations have also been investigated but no significant sensitivity found [96]. Note that any error in approximating these functions translates into an error in approximating Wagner and Kussner functions, respectively, and vice-versa; in particular, a good accuracy in approximating the formers at high reduced frequencies (i.e., highly-unsteady flow) translates into a good accuracy in approximating the latter at low reduced time (i.e., transient response), while a good accuracy at low reduced frequencies (i.e., quasi-steady flow) translates into a good accuracy at high reduced time (i.e., asymptotic response). Jones' approximations [39] deviating quite significantly from the exact curves, many other approximations are readily available in the literature [109-116] but the present ones grant the best

agreement along the entire exact curves with the least number of poles [96] (additional poles have been investigated but no significant improvement found) and possess the correct limit values (which is an essential feature for the present applications).

Noting that the gust penetration delays the circulation growth and hence reaching the asymptotic (steady) condition in Kussner's problem [21], the ratio between (modified) Sears and Theodorsen functions [23-25] may be considered as the transfer function of the gust penetration effect in the (reduced) frequency domain; therefore, the delay function $D(k)$ and $\delta(\tau)$ may suitably be defined in the (reduced) frequency and (reduced) time domains as:

$$D = \frac{C_G}{C}, \qquad \delta = \int_{-\infty}^{\infty} \frac{De^{\mathrm{j}k\tau}}{2\pi \mathrm{j}k} dk, \tag{A3}$$

respectively, as shown in Figure A2. Lastly, Figure A3 presents the application of such function to Jones' approximation [39] of the lift-deficiency function due to a unit step-change in the angle of attack and the present curve is in excellent agreement with his approximation [39] of the lift-deficiency function due to a unit step-change in the vertical speed of a "frozen" wind gust.

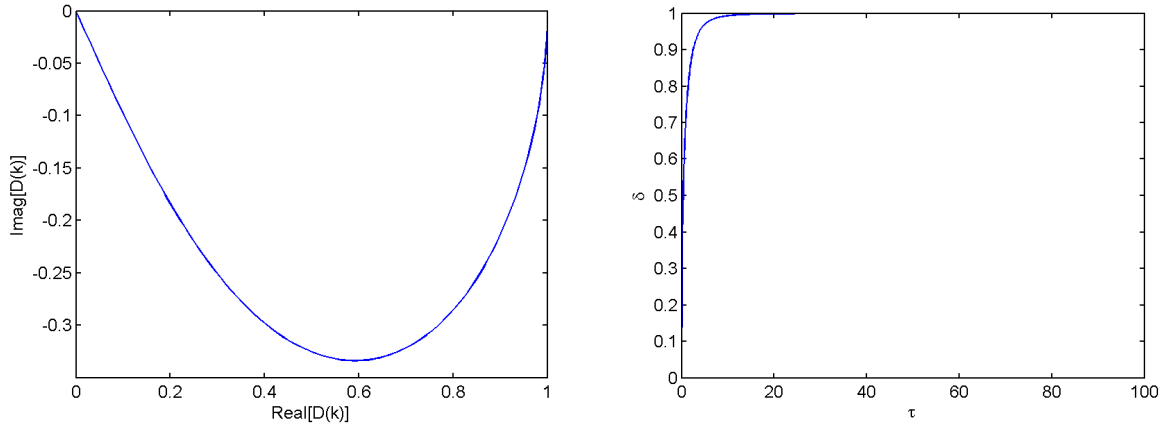

Figure A2. Delay function in the reduced frequency (left) and reduced time (right) domains

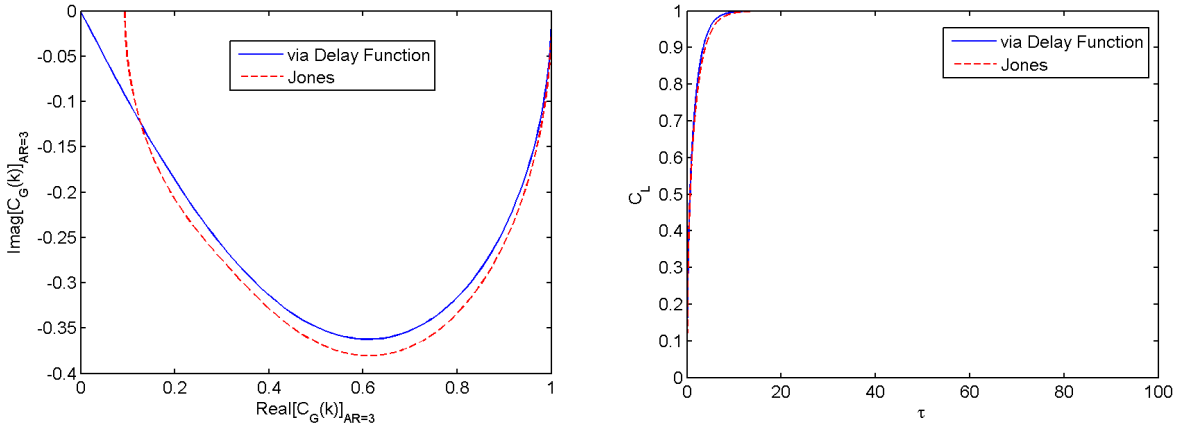

Figure A3. Approximate lift-deficiency coefficient due to a unitary sharp-edge gust for flat elliptical wing with AR=3 in the reduced frequency (left) and reduced time (right) domain

APPENDIX B. SIMPLEST PARAMETRIC APPROXIMATIONS

For thin elliptical wing [39], the simplest approximation of the lift-deficiency coefficient due to a unitary step change in the angle of attack employs a single exponential term connecting initial behaviour and asymptotic (steady) condition directly as:

$$C_L^{3D} = \frac{2\pi AR}{2+AR}\left\{1-\left[\frac{(2E-1)AR-2}{2EAR}\right]e^{-\left[\frac{2+AR}{(2E-1)AR-2}\right]\frac{\tau}{4}}\right\}, \tag{B1}$$

whereas for the case of thin rectangular wing [42] as:

$$C_L^{3D} = \frac{2\pi AR}{1+\sqrt{1+AR^2}}\left[1-\left(\frac{\sqrt{1+AR^2}-1}{2\sqrt{1+AR^2}}\right)e^{-\left(\frac{AR^2}{1+AR^2}\right)\left(\frac{\sqrt{1+AR^2}+1}{\sqrt{1+AR^2}-1}\right)\frac{\tau}{4}}\right]; \tag{B2}$$

selected curves are shown in Figure B1 and compared to those of Jones [39] and Jones [31].

As mentioned, the available steady lift coefficient for thin rectangular wings is not very accurate, due to the intrinsic limitations of the vortex-system representation employed [42]; if calculated according to lifting line theory [81,90], then the simplest approximation of the lift-deficiency coefficient due to a unitary step change in the angle of attack reads:

$$C_L^{3D} = \frac{2\pi}{1+2\pi\kappa}\left[1-\left(\frac{\sqrt{1+AR^2}-1}{2\sqrt{1+AR^2}}\right)e^{-\left(\frac{AR^2}{1+AR^2}\right)\left(\frac{\sqrt{1+AR^2}+1}{\sqrt{1+AR^2}-1}\right)\frac{\tau}{4}}\right], \tag{B3}$$

with κ shown in Figure B2 and initial behavior and asymptotic (steady) condition given by:

$$\lim_{\tau\to 0} C_L^{3D} \approx \frac{\pi\left(\sqrt{1+AR^2}+1\right)}{(1+2\pi\kappa)\sqrt{1+AR^2}}\left[1+\left(\frac{AR^2}{1+AR^2}\right)\frac{\tau}{4}\right], \qquad C_{L\infty}^{3D} = \frac{2\pi}{1+2\pi\kappa}. \tag{B4}$$

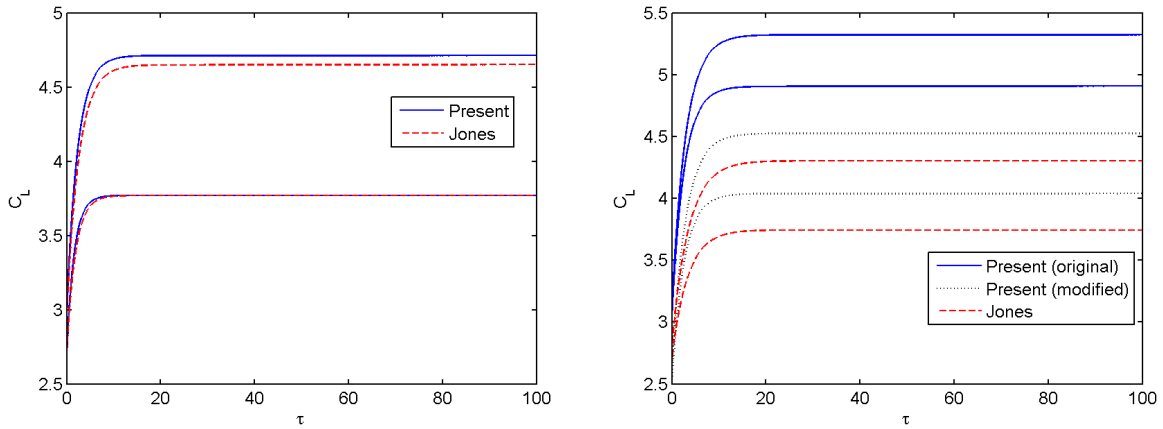

Figure B1. Lift-deficiency coefficient due to a unitary step change in the angle of attack for flat elliptical wing with AR=3,6 (left) and flat rectangular wing with AR=4,6 (right)

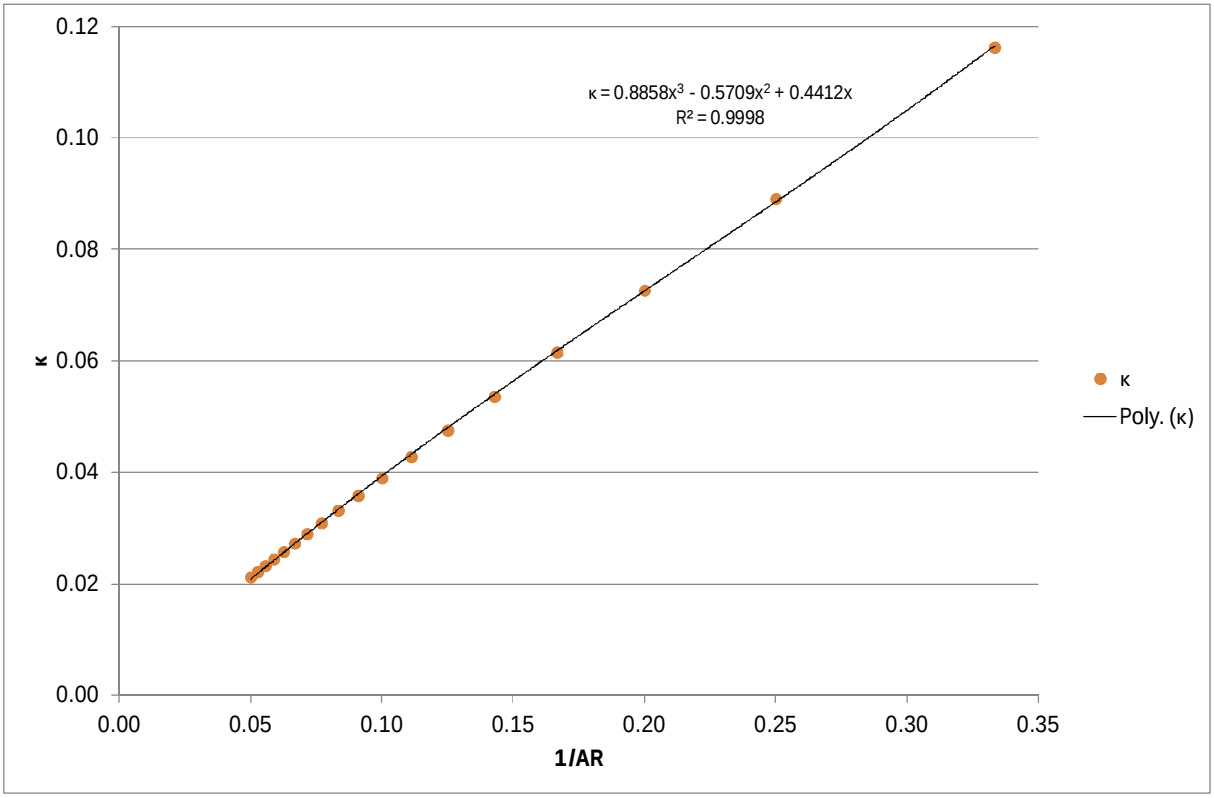

Figure B2. LLT-based coefficient for the asymptotic (steady) lift coefficient for a flat rectangular wing

REFERENCES

[1] N.M. Alexandrov, M.Y. Hussaini, *Multidisciplinary Design Optimization: State of the Art*. Proceedings in Applied Mathematics Series, SIAM, 1997.

[2] E. Kesseler, M. Guenov, *Advances in Collaborative Civil Aeronautical Multidisciplinary Design Optimization*. Progress in Astronautics and Aeronautics Series, AIAA, 2010.

[3] A. Quarteroni, G. Rozza, *Reduced Order Methods for Modeling and Computational Reduction*. Springer International Publishing, 2014.

[4] Z.Q. Qu, *Model Order Reduction Techniques with Applications in Finite Element Analysis*. Springer-Verlag, 2004.

[5] M. Gennaretti, F. Mastroddi, Study of Reduced-Order Models for Gust-Response Analysis of Flexible Fixed Wings. *Journal of Aircraft*, **41** (**2**), 2004.

[6] M. Bianchin, et al., State Space Reduced Order Models for Static Aeroelasticity and Flight Mechanics of Flexible Aircraft. *Proceedings of the 17th AIDAA Conference*, 2003.

[7] D.E. Raveh, Reduced-Order Models for Nonlinear Unsteady Aerodynamics. *AIAA Journal*, **39** (**8**), 2001.

[8] L. Cavagna, et al., Gust Loads Assessment: a Multi-Fidelity Approach. *Proceeding of the 14th IFASD*, 2011.

[9] T.M. Kier, G.H.N. Looye, Unifying Manoeuvre and Gust Loads Analysis Models. *Proceeding of the 13th IFASD*, 2009.

[10] T.M. Kier, Comparison of Unsteady Aerodynamic Modelling Methodologies with respect to Flight Loads Analysis. AIAA-2005-6027, 2005.

[11] E. Livne, The Future of Aircraft Aeroelasticity. *Journal of Aircraft*, **40** (**6**), 2003.

[12] J.R. Wright, J.E. Cooper, *Introduction to Aircraft Aeroelasticity and Loads*. AIAA Education Series, AIAA, 2007.

[13] Y.C. Fung, *An Introduction to the Theory of Aeroelasticity*. Dover, 1993.

[14] P. Marzocca, et al., Development of An Indicial Function Approach for the Two-Dimensional Incompressible/Compressible Aerodynamic Load Modelling. *Proceedings of the Institution of Mechanical Engineers, Part G: Journal of Aerospace Engineering*, **221** (**3**), 2007.

[15] E.C. Pike, Manual on Aeroelasticity. AGARD 578, 1971.

[16] M. Tobak, On the Use of the Indicial-Function Concept in the Analysis of Unsteady Motions of Wings and Wing-Tail Combinations. NACA 1188, 1954.

[17] J.G. Leishman, *Principles of Helicopter Aerodynamics*. Cambridge Aerospace Series, Cambridge University Press, 2006.

[18] R.L. Bisplinghoff, et al., *Aeroelasticity*. Dover, 1996.

[19] E.L. Houghton, et al., *Aerodynamics for Engineering Students*. Elsevier, 2012.

[20] H. Wagner, Uber die Entstenhung des dynamischen Auftriebes von Tragflugeln. *Zeitschrift für Angewandte Mathematik und Mechanik*, **5** (**1**), 1925.

[21] H.G. Kussner, Zusammenfassender Beritch uber den instationaren Auftrieb von Flugeln. *Luftfahrtforsch*, **13** (**12**), 1936.

[22] A. Kayran, Küssner's Function in the Sharp Edged Gust Problem - A Correction. *Journal of Aircraft*, **43** (**5**), 2006.

[23] T. Theodorsen, General Theory of Aerodynamic Instability and the Mechanism of Flutter. NACA 496, 1935.

[24] W.R. Sears, Operational Methods in the Theory of Airfoils in Non-Uniform Motion. *Journal of the Franklin Institute*, **230** (**1**), 1940.

[25] T. Von Karman, W.R. Sears, Airfoil Theory for Non-Uniform Motion, *Journal of the Aeronautical Sciences*, **5** (**10**), 1938.

[26] R.T. Jones, Classical Aerodynamic Theory. NASA RP 1050, 1979.

[27] B.C. Basu, G.J. Hancock, The Unsteady Motion of a Two-Dimensional Aerofoil in Incompressible Inviscid Flow. *Journal of Fluid Mechanics*, **87** (**1**), 1978.

[28] D.A. Peters, Two-Dimensional Incompressible Unsteady Airfoil Theory - An Overview. *Journal of Fluids and Structures*, **24** (**3**), 2008.

[29] F.M. Hoblit, *Gust Loads on Aircraft: Concepts and Applications*. AIAA Education Series, AIAA, 1988.

[30] W.P. Jones, Aerodynamic Forces on Wings in Simple Harmonic Motion. ARC-RM-2026, 1945.

[31] W.P. Jones, Aerodynamic Forces on Wings in Non-Uniform Motion. ARC-RM-2117, 1945.

[32] E. Reissner, Effect of Finite Span on the Airload Distributions for Oscillating Wings – Part I: Aerodynamic Theory of Oscillating Wings of Finite Span. NACA TN-1194, 1947.

[33] E. Reissner, J.E. Stevens, Effect of Finite Span on the Airload Distributions for Oscillating Wings – Part II: Methods of Calculation and Examples of Application. NACA TN-1194, 1947.

[34] H.C. Garner, Multhopp's Subsonic Lifting-Surface Theory of Wings in Slow Pitching Oscillations. ARC-RM-2885, 1956.

[35] D.E. Lehrian, Calculation of Stability Derivatives for Oscillating Wings. ARC-RM-2922, 1956.

[36] D.E. Lehrian, Calculation of Flutter Derivatives for Wings of General Planform. ARC-RM-2961, 1958.

[37] D.E. Lehrian, Initial Lift of Finite Aspect-Ratio Wings due to a Sudden Change of Incidence. ARC-RM-3023, 1957.

[38] B.D. Dore, The Unsteady Forces on Finite Wings in Transient Motion. ARC-RM-3456, 1966.

[39] R.T. Jones, The Unsteady Lift of a Wing of Finite Aspect Ratio. NACA 681, 1940.

[40] A. Hauptman, T. Miloh, Aerodynamic Coefficients of a Thin Elliptic Wing in Unsteady Motion. *AIAA Journal*, **25** (**6**), 1987.

[41] D.E. Lehrian, Vortex-Lattice Treatment of Rectangular Wings with Oscillating Control Surfaces. ARC-RM-3182, 1960.

[42] M.J. Queijo, et al., Approximate Indicial Lift Function for Tapered, Swept Wings in Incompressible Flow. NASA TP-1241, 1978.

[43] D.E. Lehrian, Aerodynamic Coefficients for an Oscillating Delta Wing. ARC-RM-2841, 1957.

[44] E. Albano, W.P. Rodden, A Doublet-Lattice Method for Calculating the Lift Distribution of Oscillating Surfaces in Subsonic Flows. *AIAA Journal*, **7** (**2**), 1969.

[45] F. Woodward, An Improved Method for the Aerodynamic Analysis of Wing-Body-Tail Configurations in Subsonic and Supersonic Flow. NASA CR-2228, 1973.

[46] L. Morino, A General Theory of Unsteady Compressible Potential Aerodynamics. NASA CR-2464, 1974.

[47] J. Katz, A. Plotkin, *Low Speed Aerodynamics*. Cambridge University Press, 2001.

[48] J.A. Drischler, Approximate Indicial Lift Function for Several Wings of Finite Span in Incompressible Flow as obtained from Oscillatory Lift Coefficients. NACA TN-3639, 1956.

[49] C. Scruton, et al., Measurements of the Aerodynamic Derivatives for Swept Wings of Low Aspect Ratio describing Pitching and Plunging Oscillations in Incompressible Flow. ARC-RM-2925, 1957.

[50] G.F. Moss, Low-Speed Wind-Tunnel Measurements of Longitudinal Oscillatory Derivatives on Three Wing Plan-forms. ARC-RM-3009, 1957.

[51] I.H. Abbott, A.E. von Doenhoff, *Theory of Wing Sections: Including a Summary of Airfoil Data*. Dover, 1959.

[52] J.G. Leishman, Indicial Lift Approximations for Two-Dimensional Subsonic Flow as Obtained from Oscillatory Measurements. *Journal of Aircraft*, **30** (**3**), 1993.

[53] M. Gaunaa, et al., Indicial Response Function for Finite-Thickness Airfoils, a Semi-Empirical Approach. AIAA-2011-542, 2011.

[54] T.J. Chung, *Computational Fluid Dynamics*. Cambridge Press, 2002.

[55] L. Cavagna, et al., Efficient Application of CFD Aeroelastic Methods Using Commercial Software. *Proceedings of the 11th IFASD*, 2005.

[56] G. Romanelli, et al., A "Free" Approach to Computational Aeroelasticity. AIAA-2010-176, 2010.

[57] A. Da Ronch, et al., On the Generation of Flight Dynamics Aerodynamic Tables by Computational Fluid Dynamics. *Progress in Aerospace Sciences*, **47**, 2011.

[58] M. Ghoreyshi, et al., Reduced Order Unsteady Aerodynamic Modeling for Stability and Control Analysis Using Computational Fluid Dynamics. *Progress in Aerospace Sciences*, **71**, 2014.

[59] V. Parameswaran, J.D. Baeder, Indicial Aerodynamics in Compressible Flow-Direct Computational Fluid Dynamic Calculations. *Journal of Aircraft*, **34** (**1**), 1997.

[60] W. Silva, Discrete-Time Linear and Nonlinear Aerodynamic Impulse Responses for Efficient Use of CFD Analyses. *PhD Thesis*, College of William & Mary, 1997.

[61] M. Ghoreyshi, et al., Computational Investigation into the Use of Response Functions for Aerodynamic-Load Modeling. *AIAA Journal*, **50** (**6**), 2012.

[62] P.G.A. Cizmas, J.I. Gargoloff, Mesh Generation and Deformation Algorithm for Aeroelasticity Simulations. *Journal of Aircraft*, **45** (**3**), 2008.

[63] C.D. Wieseman, Methodology for Matching Experimental and Computational Aerodynamic Data. NASA TM-100592, 1988.

[64] G. Dhatt, et al., *Finite Element Method*. Wiley, 2013.

[65] K.J. Bathe, *Nonlinear Finite Element Analysis and ADINA*. Pergamon Press, 1977–1999.

[66] C. Farhat, et al., Load and Motion Transfer Algorithms for Fluid/Structure Interaction Problems with Non-Matching Discrete Interfaces: Momentum and Energy Conservation, Optimal Discretization and Application to Aeroelasticity. *Computer Methods in Applied Mechanics and Engineering*, **157** (**1-2**), 1998.

[67] C. Farhat, V. Lakshminarayan, An ALE Formulation of Embedded Boundary Methods for Tracking Boundary Layers in Turbulent Fluid-Structure Interaction Problems. *Journal of Computational Physics*, **263**, 2014.

[68] J.G. Leishman, K.Q. Nguyen, State-Space Representation of Unsteady Airfoil Behavior. *AIAA Journal*, **28** (**5**), 1990.

[69] M. Meyer, H.G. Matthies, State-Space Representation of Instationary Two-Dimensional Airfoil Aerodynamics. *Journal of Wind Engineering and Industrial Aerodynamics*, **92** (**3-4**), 2004.

[70] G.N. Vanderplaats, *Numerical Optimization Techniques for Engineering Design: with Applications*. Series in Mechanical Engineering, McGraw Hill, 1984.

[71] S.H. Tiffany, W.M. Adams, Nonlinear Programming Extensions to Rational Function Approximation Methods for Unsteady Aerodynamic Forces. NASA-TP-2776, 1988.

[72] K.L. Roger, Airplane Math Modeling Methods for Active Control Design, AGARD-CP-228, 1977.

[73] R. Vepa, Finite State Modeling of Aeroelastic System. NASA-CR-2779, 1977.

[74] H. Dunn, An Analytical Technique for Approximating Unsteady Aerodynamics in the Time Domain. NASA-TP-1738, 1980.

[75] T.S. Beddoes, Practical Computation of Unsteady Lift. *Vertica*, **8** (**1**), 1984.

[76] M. Karpel, E. Strul, Minimum-State Unsteady Aerodynamic Approximations with Flexible Constraints, *Journal of Aircraft*, **33** (**6**), 1996.

[77] I. Cotoi, R.M. Botez, Method of Unsteady Aerodynamic Forces Approximation for Aeroservoelastic Interactions. *Journal of Guidance, Control and Dynamics*, **25** (**5**), 2002.

[78] R.B. Holmes, *A Course on Optimization and Best Approximation*. Lecture Notes in Mathematics, Springer, 1972.

[79] D. Poirel, Random Dynamics of a Structurally Nonlinear Airfoil in Turbulent Flow. *PhD Thesis*, McGill University, 2001.

[80] A. Quarteroni, et al., *Numerical Mathematics*. Springer-Verlag, 2000.

[81] J.D. Anderson, *Fundamentals of Aerodynamics*. McGraw-Hill, 2007.

[82] A. Sedaghat, et al., Curve Fitting Approach for Transonic Flutter Prediction. *The Aeronautical Journal*, **107** (**1075**), 2003.

[83] J. Brink-Spalink, J.M. Bruns, Correction of Unsteady Aerodynamic Influence Coefficients Using Experimental or CFD Data. AIAA-2000-1489, 2000.

[84] R. Palacios, et al., Assessment of Strategies for Correcting Linear Unsteady Aerodynamics Using CFD or Test Results. *Proceedings of the 9th IFASD*, 2001.

[85] D. Dimitrov, R. Thormann, DLM-Correction Method for Aerodynamic Gust Response Prediction. *Proceedings of the 15th IFASD*, 2013.

[86] M. Berci, et al., Dynamic Response of Typical Section Using Variable-Fidelity Fluid Dynamics and Gust-Modeling Approaches - With Correction Methods. *Journal of Aerospace Engineering*, **27** (**5**), 2014.

[87] R. Jin, et al., Comparative Studies of Metamodelling Techniques under Multiple Modelling Criteria. *Journal of Structural Optimisation*, **23** (**1**), 2001.

[88] J.B. Hiriart-Urruty, *Optimization: Theory and Algorithms*. Dekker, 1983.

[89] C.T. Leondes, *Optimization Techniques*. Elsevier, 1998.

[90] Prandtl, L., Applications of Modern Hydrodynamics to Aeronautics. NACA TR-116, 1921.

[91] D.A. Peters, et al, Finite State Induced Flow Models – Part I: Two-Dimensional Thin Airfoils. *Journal of Aircraft*, **32** (**2**), 1995.

[92] D.A. Peters, et al, A State-Space Airloads Theory for Flexible Airfoils. *Journal of the American Helicopter Society*, **52** (**4**), 2007.

[93] L.E. Garrick, On some Reciprocal Relations in the Theory of Nonstationary Flows. NACA-629, 1938.

[94] M.A. Heaslet, J.R. Spreiter, Reciprocity Relations in Aerodynamics. NACA-1119, 1953.

[95] G.M. Graham, Aeroelastic Reciprocity: An Indicial Response Formulation. AFOSR-TR-95, 1995.

[96] M. Berci, Optimal Approximations of Indicial Aerodynamics. *Proceedings of the 1st OPTi*, 2014.

[97] B.O. Peirce, *A Short Table of Integrals*. Ginn & Company, 1929.

[98] M.W. Kutta, Auftriebskräfte in Strömenden Flüssigkeiten. *Illustrierte Aeronautische Mitteilungen*, **6** (**133**), 1902.

[99] N.E. Joukowski, Sur les Tourbillons Adjionts. *Traraux de la Section Physique de la Societé Imperiale des Amis des Sciences Naturales*, **13** (**2**), 1906.

[100] H. Glauert, *The Elements of Aerofoil and Airscrew Theory*. Cambridge University Press, 1947.

[101] T. Van Holten, Some Notes on Unsteady Lifting-Line Theory. *Journal of Fluid Mechanics*, **77** (**3**), 1976.

[102] P.D. Sclavounos, An Unsteady Lifting-Line Theory. *Journal of Engineering Mathematics*, **21** (**3**), 1987.

[103] J.L. Guermond, A. Sellier, A Unified Unsteady Lifting-Line Theory. *Journal of Fluid Mechanics*, **229**, 1991.

[104] W.P. Rodden, *Theoretical and Computational Aeroelasticity*. Crest Pub., 2011.

[105] C.F.J. Wu, M. Hamada, *Experiments: Planning, Analysis, and Parameter Design Optimization*. Series in Probability and Statistics, Wiley, 2009.

[106] J.A. Nelder, R. Mead, A Simplex Method for Function Minimization. *Computer Journal*, **7**, 1965.

[107] M. Affenzeller, *Genetic Algorithms and Genetic Programming in Practice: Efficient Algorithm-Design in a Flexible Development Platform*. Chapman & Hall, 2009.

[108] U. Gulcat, *Fundamentals of Modern Unsteady Aerodynamics*. Springer, 2011.

[109] R. Vepa, On the Use of Pade' Approximants to Represent Unsteady Aerodynamic Loads for Arbitrarily Small Motions of Wings. AIAA-76-17, 1976.

[110] R.N. Desmarais, A Continued Fraction Representation for Theodorsen's Circulation Function. NASA-TM-81838, 1980.

[111] E.H. Dowell, A Simple Method for Converting Frequency Domain Aerodynamics to the Time Domain. NASA-TM-81844, 1980.

[112] C. Venkatesan, P. Friedmann, New Approach to Finite-State Modeling of Unsteady Aerodynamics. *AIAA Journal*, **24** (**12**), 1986.

[113] L.D. Peterson, E.F. Crawley, Improved Exponential Time Series Approximations of Unsteady Aerodynamic Operators. *Journal of Aircraft*, **25** (**2**), 1988.

[114] W. Eversman, A. Tewari, Modified Exponential Series Approximation for the Theodorsen Function. *Journal of Aircraft*, **28** (**9**), 1991.

[115] A. Tewari, J. Brink-Spalink, Multiple Pole Rational-Function Approximations for Unsteady Aerodynamics. *Journal of Aircraft*, **30** (**3**), 1993.

[116] S.L. Brunton, C.W. Rowley, Empirical State-Space Representations for Theodorsen's Lift Model. *Journal of Fluids and Structures*, **38** (**1**), 2013.